Proposal for the Hall-D Beam Line Pair Spectrometer - Goals, Technical Description, and Specifications

1) Introduction

The photon beam source for Hall-D will be based on coherent bremsstrahlung of the CEBAF 12GeV beam with a diamond radiator. The photon beam generated by the interaction with the diamond radiator will consist of contributions both of incoherent un-polarized bremsstrahlung photons and partially linearly polarized coherent bremsstrahlung photons. As the angular divergence of the incoherent component is larger than the coherent component, the coherent component can be enriched by collimation after a large drift space. It is planned to place the primary collimator for Hall-D 76m downstream of the diamond radiator which corresponds to about 30 m in front of the GlueX detector. A tagging spectrometer, referred to as the tagger, will be built 2m downstream of the radiator and will measure the energy of the electrons which radiated the photons, the photon energy will then determined from energy conservation. The tagger will be readout for every GlueX trigger and will be the primary measurement of the photon energy. Additionally the tagger can be readout using a random bunch crossing in order to measure the photon energy spectrum of the uncollimated photon beam $I_\gamma^{uncoll}(E)$. Cross section measurements at GlueX will require in addition a measurement of the photon flux as a function of energy of the beam after the collimators, $I_\gamma^{coll}(E)$. In principle the photon spectrum could be determined by the GlueX detector from the measured trigger rates. However this would require understanding the acceptance and trigger efficiencies at the 1-2% level. In practice, an additional instrument will be needed for a precise measurement of the photon flux incident on the GlueX target. In addition to the absolute flux measurement, the linear polarization of the photon beam also needs measured.

In order to have a precision measurement of the characteristics of the photon beam it is necessary to base the measurement on a well understood process. It is proposed to use pair production which is a well understood QED process as the basis for the luminosity measurement and polarization determination. The pair production cross section between E_γ of 12 and 5 GeV is accurate to 0.XX%. In this document a pair spectrometer is proposed based on a single magnet and a simple detector array. A single simple magnet design is chosen to minimize the uncertainty in the magnetic field seen by the electron and positron. The pair spectrometer is self calibrating to the extent that the absolute energy scale can be determined from the high energy edge of the photon spectrum. The endpoint of the spectrum corresponds to the CEBAF beam energy which is known to better than 10^{-4}. The beam flux $I_\gamma^{coll}(E)$ is determined from the coincidence rates in the spectrometer. The excellent energy calibration of the pair spectrometer will allow a cross calibration of the photon energy measurement in the tagger spectrometer by looking at coincidences between the two spectrometers. This technique can also be used to determine the tagger trigger efficiency. Finally a careful analysis of the flux function $I_\gamma^{coll}(E)$ can determine the polarization of the photon beam. In summary the goals for this Pair Spectrometer are as follows:

a) Continuously measure the beam flux as a function of energy $I_\gamma^{coll}(E)$ between 6 and12 GeV
b) Determine the photon beam linear polarization
c) Provide an independent tagger energy calibration
d) Measure the tagger trigger efficiency

In addition to the above goals the pair spectrometer must be designed so that the spectrometer can be upgraded in the future with silicon detectors to measure the photon beam linear polarization directly. This requires a minimum of 1m drift space between the pair spectrometer radiator and the magnet.

2) Pair Spectrometer Design

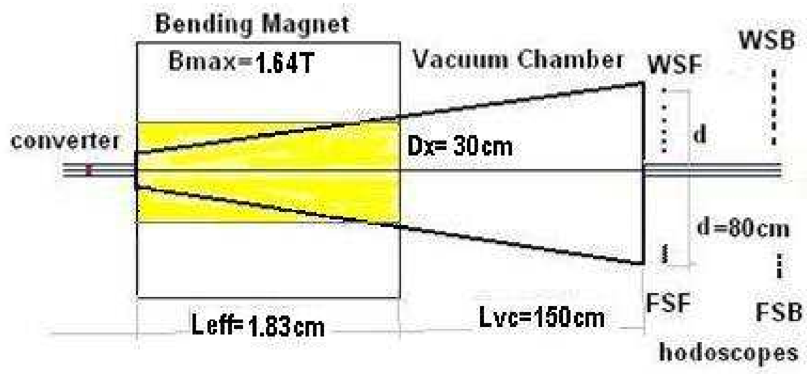

Figure 1 Layout of the proposed pair spectrometer. On the left is a thin 10^{-4} converter followed by a strong spectrometer magnet. The vacuum chamber extends 1.5 m beyond the end of the magnet. Immediately outside the vacuum chamber is a hodoscope detector.

The layout of the pair spectrometer is shown in Figure 1. The photon beam is sampled with a thin converter shown on the left of Figure 1. As the pair production cross section is large a thin radiator can be used. The optimum choice for the radiator thickness will depend on the details of the detector design and photon beam flux and will therefore be discussed after the detector is described. The target holder will be positioned at least 1m upstream of the pair spectrometer magnet and will be equipped with several different thickness radiators. The converter ladder can also be completely removed from the beam.

The design of the pair spectrometer magnet and vacuum chamber are coupled. The weaker the magnet the longer the vacuum chamber needs to be. The optimum design is one where 12 GeV electrons or positrons will pass through an exit window at the end of the vacuum chamber and strike a shielding wall downstream of the spectrometer. This design guarantees that the spectrometer will have a minimum amount of background and it will not disturb the GlueX data taking. The pole tip of the magnet must be wide enough not to block the low energy particles of interest and the magnet should operate at a field where the iron is not saturated, so the field will be reproducible at 1 in 10-4. For this study a magnet with an effective length L_{eff}= 1.829m, an integrated field strength Int[B*dL] =2.991T*m, an operating field B_{max}=1.64tesla, and a pole width D_x=±30cm is assumed. With this magnet the vacuum chamber must extend 1.5m beyond the end of the magnet. With this design 12 GeV electrons or positrons will exit the vacuum chamber xcm from photon beam axis leaving sufficient space for a flange for the photon beamline and the exit window mount. The vacuum chamber is constructed of non-magnetic material (aluminum or stainless steel) and is 160 cm wide at the downstream end. This allows particle deflected by up to 17° to be detected and is matched to the pole tip width.

The scintillator hodoscope detectors are shown on the right in Figure 1. The Fine Spacing Forward (FSF) hodoscope (positron arm) and Wide Spacing Forward (WSF) hodoscope (electron arm) are used to measure the energy while the Fine Spacing Backward hodoscope (FSB) and Wide Spacing Backward hodoscopes (WSB) are used for triggering purposes. The hodoscopes are designed to provide uniform acceptance over the energy range of 12.4GeV to 6.4GeV. The FSF hodoscope is a single layer close packed scintillator hodoscope with fine segmentation. The FSF hodoscope will consist of 24 channels and will cover the positron momentum range of either 3-4GeV. The segmentation of the FSF determines to a large extent the energy resolution of the pair spectrometer. The WSF hodoscope is a set of six narrow scintillators positioned to detect electrons with step of 1GeV/c from 3.25 to a 8.25 GeV. The detector arms are taken in coincidence and the photon energy is the sum of the positron and electron energies.

This combination of detectors then covers the momentum range of 6.25 to 12.21 GeV. As the momentum range in the FSF hodoscope is the same as the gap between the WSF this arrangement of detectors provides a uniform acceptance over the measured range. This design of a minimal-overlapping spectrometer is also a cost effective way to cover the desired momentum range. In this design the width of the energy bins is determined by the size of the fine spaced hodoscope ($\Delta E_\gamma = \Delta P_+$). The number of energy bins per GeV needs to be selected as fine as the corresponding distortion of the coherent bremsstrahlung spectrum does not dominate the uncertainty in the determination of the linear polarization of the beam as determined fron the shape analysis. As seen in Figure 2, already 15 bins per GeV gives a fairly accurate determination of the shape, while in presented design an option of 24bins/GeV is considered. Detailed studies are necessary to determine the optimum binning.

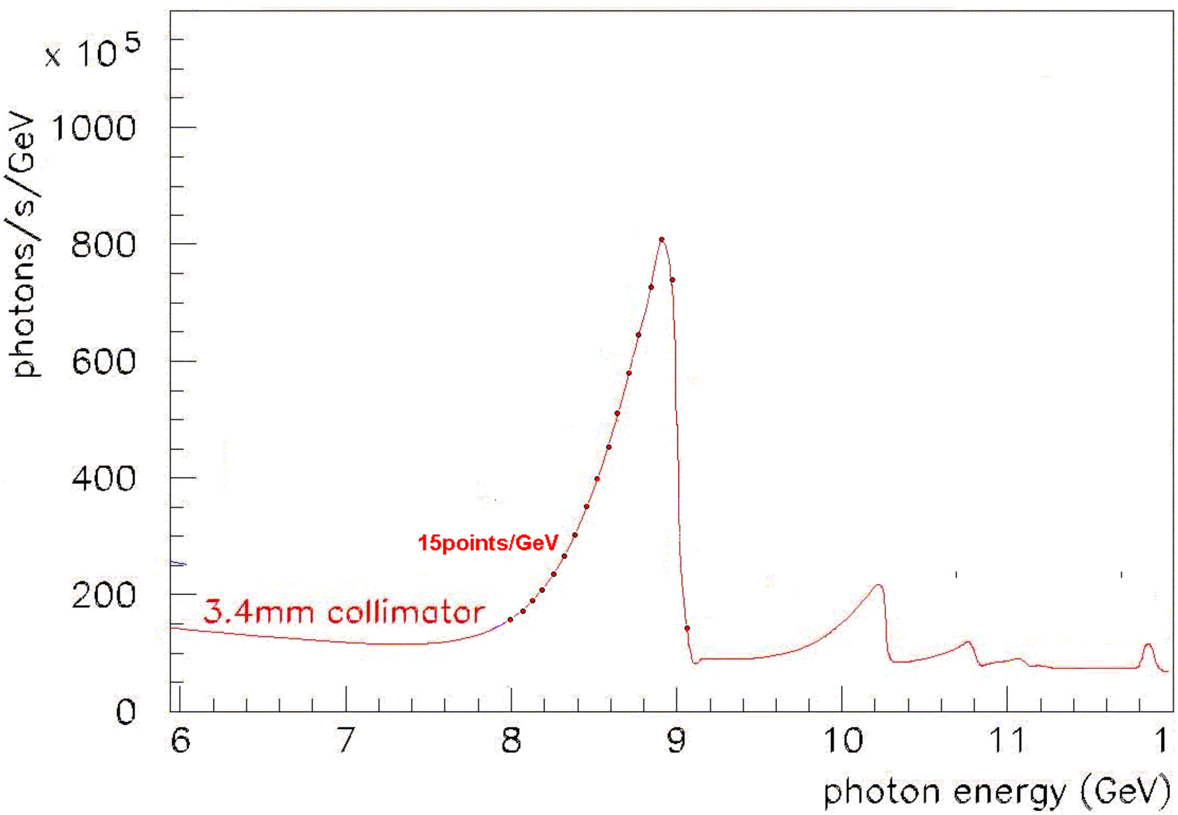

Figure 2 Typical photon energy spectra are shown for a 3.4mm collimator. Superimposed on the curves are the energy measurement points corresponding to a FSF hodoscope with either 10 or 15 scintillators.

Experimental factors such as the beam spot size on the pair spectrometer converter, the opening angle for the e+/e- pair coming from the pair production cross section, and multiple scattering effects in the radiator and exit window will determine the optimum granularity of the FSF scintillators.

If a higher photon energy resolution is required than what is possible from the FSF hodoscope alone then the widths of the WSF hodoscope scintillators can be reduced. The energy resolution is given in the expression below:

$$(\sigma_\gamma / E_\gamma) = (\sigma_+^2 + \sigma_-^2)^{1/2} / (P- + P+)$$

where σ_γ is the width of the reconstructed photon energy distribution for a given bin, E_γ the central energy, σ_+ and σ_- are the uncertainties in the positron and electron energies, and P- and P+ the positron and electron momentum. **To prevent the strong overlap of the neighbor bins, an acceptable energy resolution σ_γ is selected at least equal to a half of the bin size ($\sigma_\gamma \leq \Delta E_\gamma/2$.**. Reducing the width of the WSF hodoscope to increase the energy resolution has an immediate impact on the pair spectrometers' already low acceptance. This is especially important at the high energy end of the photon spectrum where the rate is dropping rapidly.

One possible hodoscope design based on the assumption of a 1.83m long magnet with B=1.64T field and 600mm wide poles is shown in the following Tables 1,2.

Counters of WSF hodoscope	P GeV/c	Electron bending angle deg	Radius of curvature M	Distance to beam line cm	Scintillator width for σ_γ=21.7MeV cm
WSF1	3.25	16.03	6.62	68.8	1.31
WSF2	4.25	12.19	8.66	51.9	0.75
WSF3	5.25	9.84	10.69	45.4	0.54
WSF4	6.25	8,25	12.75	35.0	0.35
WSF5	7.25	7.11	14.78	30.1	0.25
WSF6	8.25	6.24	16.83	26.4	0.2

Table 1: Detailed summary of the wide spaced forward (WFS) hodoscope detectors.

Minimum momentum	3.0 GeV
Maximum momentum	3.96 GeV
Number of scintillators	24
Momentum range per scintillator	δP=0.0435GeV/c
Radius of curvature	R= 6.12– 8.09m
Deflection angle	α=17.4 – 13.1^o
Distance to beam axis	x=55.9 – 75cm
Total FSF pack width	19.1cm
Single channel width	$<\delta x> = \Delta x/(Ns-1)=0.83$cm

Table 2: Detailed summary of the fine spaced forward (FSF) hodoscope. In this design 63 MeV/c momentum bins are used.

Looking at the widths of the strips in the WSFH arm Table 1 column 6 one sees that the width of the counters decreases as the momentum increases. This is necessary to match the momentum spread in the WSF to the photon energy resolution at fixed one in FSF arm. **The strip width defined by requested resolution, is less at smaller deflections (higher momentum), so having selected a resolution in aFSF arm, one automatically selects a comparable resolution in a WSF arm.**

E_γ range*GeV)	6-7	7-8	8-9	9-10	10-11	11-12
Widths of WSF strips convoluted with beam spot size.(cm)	1.353	0.82	0.64	0.49	0.42	0.4
σ_γ(corrected) (MeV)	23.2	24.0	25.5	28.7	32.2	38.1

Table3. Summary on WSF strips' effective width (beam spot size convoluted) and . impact to a photon energy resolution.

The position spread is caused mainly by the beam spot size of 3.4mm on the radiator but multiple scattering in the radiator and the small transverse momentum spread in the pair production process also contribute. An impact of the beam spot size to a photon energy resolution through the "effective" WSF strips widths size is shown in Table 3. This position uncertainty dominate the energy resolution at large energies. In the region of the peak of the coherent bremsstrahlung (P_- = 5.25GeV and P_+ ranges between 3 and 3.96GeV) the effect of the beam spot size on the energy resolution is 18%(25.5 MeV instead of uniform 21.7MeV over full energy range expected)..

The details of backward layer hodoscopes are not presented here because the studies to understand if they are needed are still underway and will depend on background rate estimates. However similar trigger hodoscopes are in use in the Hall-B air spectrometer and are important for cleaning-up the noisy background. Their need in the Hall-D PS may be also be indirectly confirmed from Hall B's data on single arm and coincidence rates. The geometry of the backward layer hodoscopes is shown in PS layout above and is used for the design of the PS trigger scheme presented below. The present backward hodoscopes consist of consists of 6 strips behind the WSF hodoscope and 3 strips behind the FSF hodoscopes. The trigger hodoscope arrays are located 1m downstream, behind WSF (6) and FSF (16) hodoscopes respectively.

3) Pair spectrometer projected performance

a) Energy resolution, efficiency and rates

The energy resolution for FSF granularity 16 and 24 with beam spot size accounted are compared for the optimal choice. The following results are obtained:

	E_γ = 8-9 GeV		E_γ= 11-12GeV	
	n=16	n=24	n=16	n=24
σ_γ(MeV)	35.6	25.5	45.8	38.1

There is an essential gain in photon resolution below 10GeV for FSF granularity n=24 while at the high energy end of the bremmstrahlung the beam spot size mostly dominates and equalize the resolution in cases considered. If one increase the widths of WSF(5,6) to 0.4cm for efficiency gain, the photon energy resolutions become 51.7 and 49.5MeV for n=16 and 24 bins respectively.

The efficiency for each photon energy bin defined by a two arm coincidence has to be accurately determined. **The relative efficiency of PS channels can be directly measured using a bremsstrahlung spectrum that has a known shape. An amorphous radiator installed in goniometer will supply PS by collimated incoherent radiation, that allows to extract efficiency for each channel comparing the measured and calculated energy spectrum.** This procedure should be regularly repeated in order to monitor and correct any possible instability. The absolute efficiency of PS can be measured experimentally at a known flux using the total absorption counter.

The rates in the PS were evaluated as the product of the momentum phase space coverage in both arms at a few photons energy. The acceptance was found to be approximately 0.1%/GeV on average, decreasing toward high energy end of bremsstrahlung spectrum (0.15% at 6GeV, 0.1% at 9GeV and 0.08% at 12GeV). With this acceptance and assuming 100% detector efficiency an expected rate in the region of the coherent bremsstrahlung peak is on the order of 100 Hz at a converter thickness selected to be $\sim 10^{-3}$ radiation lengths and a photon flux of $\sim 10^{8}$.

At known end point energy precision better that $>10^{-4}$ (~10MeV), its shape, measured by PS, is smeared out with PS resolution (~50MeV) and can be fitted to Gaussian with FWHM energy point attributed to 12 GeV).

The granularity of CB spectrum the pair spectrometer is 43 MeV as determined by the FSF hodoscope. The error on this measurement will depend on the accuracy of the scintillator manufacture, placement accuracy of the scintillators, the precision of the field map and the beam spot size on the radiator. This will need studied in more detail.

b) Tagger calibration

As an instrument with simple configuration the energy of the photons can accurately be determined using the pair spectrometer. Therefore it can be used as a reference to cross calibrations of the tagger spectrometer which has more complicated configuration and operates at a much higher rate ($>10^{11}$). The tagger spectrometer measures the energy of the photons in the beam by measuring the energy loss of the electrons and the pair spectrometer measures the energy of a small fraction of these photons which undergo pair production in the PS radiator. By looking at the events where a coincidence exists between the tagger and the pair spectrometer these two energy measurements can be compared. A typical cross-check of the photon energy measured in PS and the tagger is shown in scatter-plot in Figure 3. Each point in the plot is the combination of PS and tagger measurement with the relevant error bars of corresponding energy resolutions.

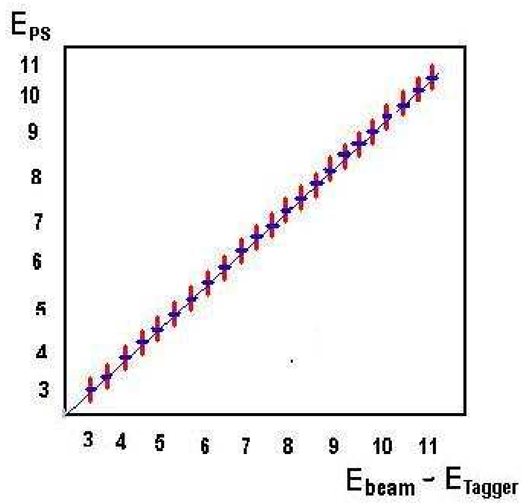

Figure 3: Cross calibration of the tagger using the pair spectrometer.

In this plot the energy resolution of the tagger is higher than that of the PS but this does not affect the precision of the cross-check if enough statistics are accumulated for each tagger's energy bin which allows the determination of the local PS spectrum mean with a precision comparable to tagger resolution and then make a cross-check of tagger energy.

Note this plot may contain information on the random coincidence inside of each of devices and between them, that affects the measured energy and the corresponding point in plot is shifted out of the calibration line in parallel to a related axes . Please explain last sentence

c) Photon beam linear polarization determination

The measurement of the CB spectrum allows to exploit the size and shape of the CB peak to calculate the linear polarization. The methods developed for this task are quite advanced and require only the wide enough measured energy range above and below the peak region. (Insert reference) For example at peak energy setting at 9 GeV, the range from 6 to 12 GeV is quite appropriate for this task, allowing the reachable precision to be in order of 0.01-0.02 in the working range $(E-E_{peak})/E_{peak}<0.3$. Outside of this range the polarization is low and compatible with zero.

d) Electronics

The entire pair spectrometer consist of a total of 42 counters: FSF(24),FSB(4),WSF(6),WSB(6). The proposed readout and trigger schemes for the detector are shown in Figures 4,5 and 6. The scintillators are read out using photomultiplier tubes which are powered by a CAEN SY2527 based system. The signals from the FSF and WSF are discriminated using CAEN V812 constant fraction discriminators, while backward layer hodoscopes are readout by ordinary discriminators. The signals are then digitized using the fTDC. The outputs of the FSB and WSB hodoscopes are directly connected to a fADC250 running in hit bit mode and PS trigger hit is elaborated as a fast coincidence between two PS arms at data fast data processing. . The trigger hit pattern is then transported via CTP and SSP modules to the global trigger processor (GTP) where the pair spectrometer trigger is formed.

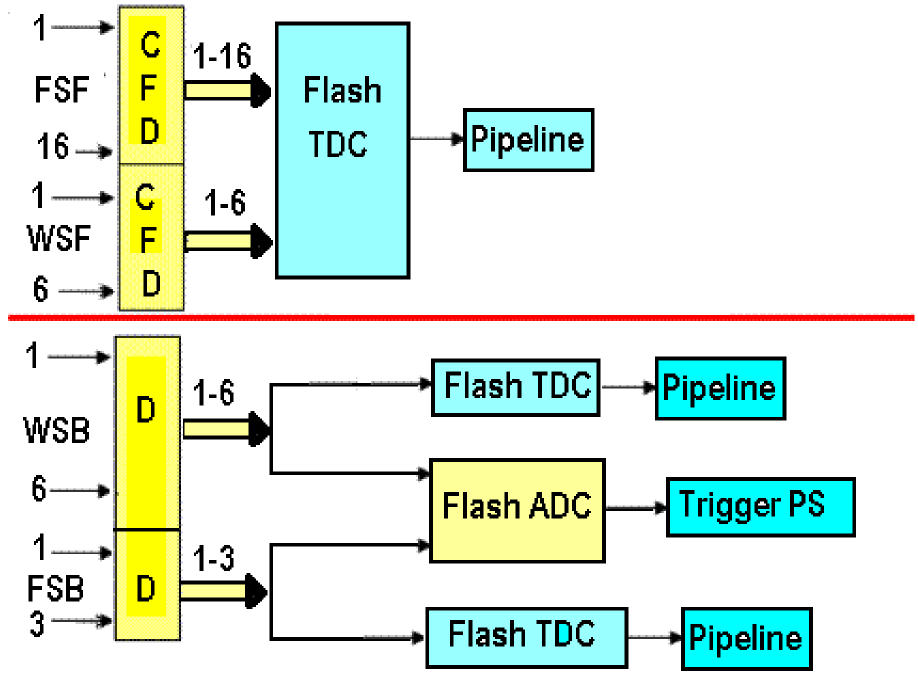

Figure 4 Sketch of the proposed electronics.

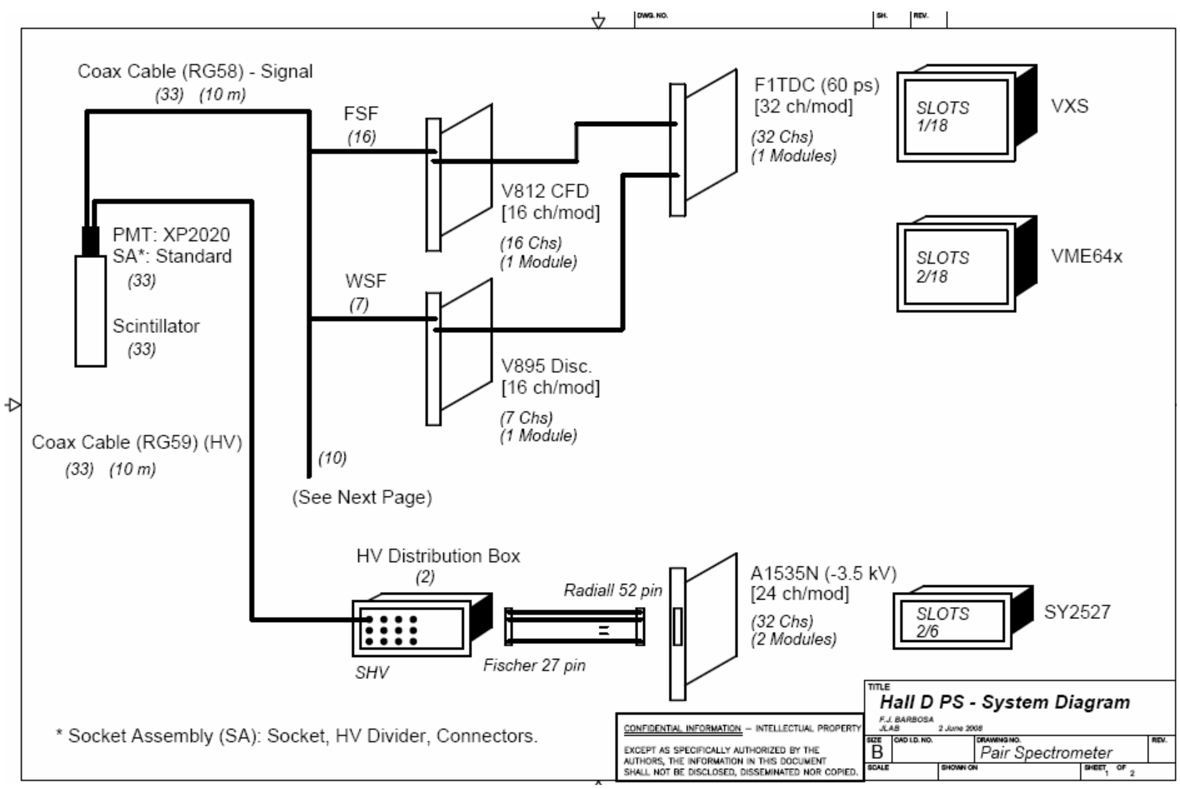

Figure 5: Readout scheme for the pair spectrometer.

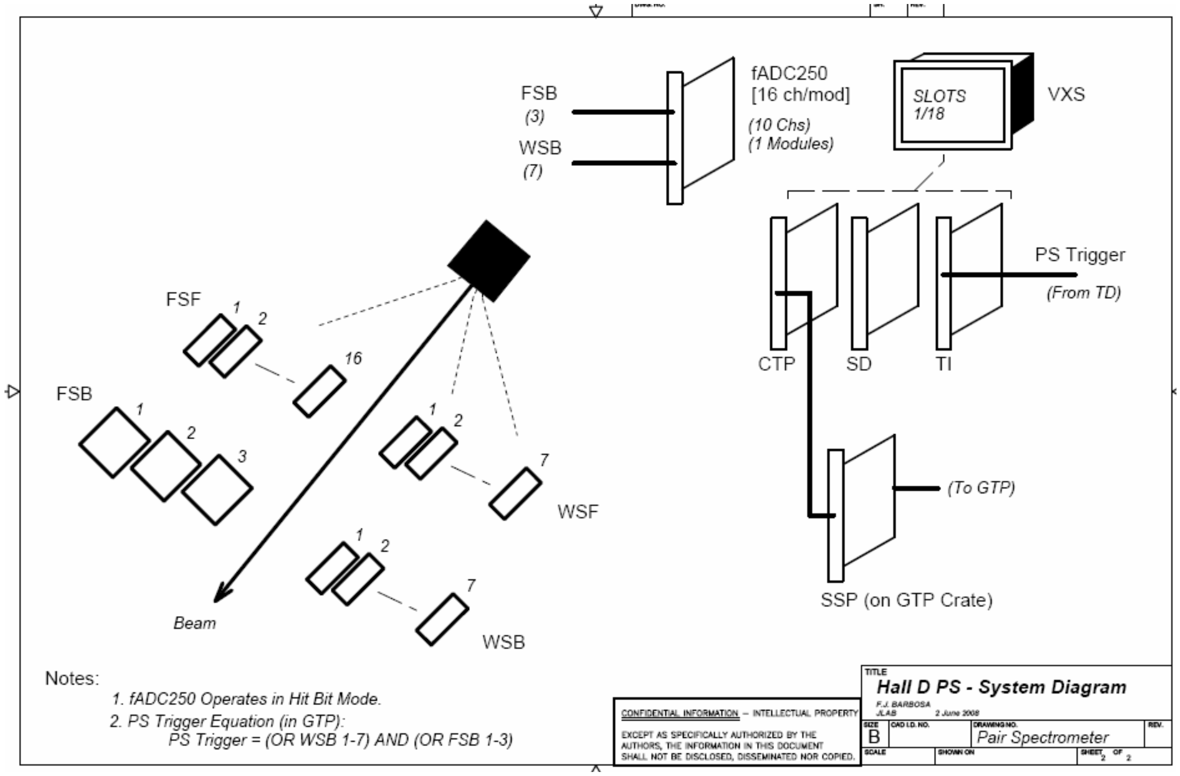

Figure 6: Trigger scheme for the pair spectrometer

e) Software

The software for PS should imply:
- measurements of PS efficiency using incoherent bremmstrahlung spectra
- search of crystal axes orientation in angular scan
- online measurements and monitoring of CB spectra with feedback to crystal positioning.
- off-line PS data analysis and CB polarization calculation

All these programs were developed for YERPHI's γ-2 linearly polarized beamline facility and can be adopted to Hall D's special requirements and conditions .

f) Work to do: First steps

1.To look for the relevant dipole magnet and make his trajectories precise calculations for detectors layout arrangement using magnet field topography. The full simulations of pair production process for 9GeV photons in selected PS layout to see its performance: resolutions and efficiencies.
2.To select the counters structure: scintillator type, light guides, PMT's..
3. To design the mechanical structures of PS detectors : hodoscopes and counters, located at the movable supports on the rails for the precise adjustments with relevant references and measurement means, holders of PMT with magnetic shielding inside.
4. To select the quality checks of the components and start their design and prototyping. Preparation of the test benches for certification of hodoscopes and counters after assembly.

We are able to do these steps